Inhibition of non-Hermitian topological phase transitions in sliding photonic quasicrystals

STEFANO LONGHI[1,2,*]

[1] Dipartimento di Fisica, Politecnico di Milano, Piazza L. da Vinci 32, I-20133 Milano, Italy
[2] IFISC (UIB-CSIC), Instituto de Fisica Interdisciplinar y Sistemas Complejos - Palma de Mallorca, Spain
[*] stefano.longhi@polimi.it

Compiled October 8, 2023

Non-Hermitian (NH) quasicrystals have been a topic of increasing interest in current research, particularly in the context of NH topological physics and materials science. Recently, it has been suggested and experimentally demonstrated using synthetic photonic lattices that a class of NH quasicrystals can feature topological spectral phase transitions. Here we consider a NH quasicrystal with a uniformly-drifting (sliding) incommensurate potential and show that, owing to violation of Galilean invariance, the topological phase transition is washed out and the quasicrystal is always in the delocalized phase with an entirely real energy spectrum. The results are illustrated by considering quantum walks in synthetic photonic lattices.

http://dx.doi.org/10.1364/ao.XX.XXXXXX

Quasicrystals are special structures that exhibit long-range order but lack translational symmetry [1]. Owing to the presence of non-crystallographic symmetry, quasicrystals have unique properties, such as metal-insulating phases and mobility edges, which can be described by Hermitian tight-binding Hamiltonians with incommensurate potentials [2]. Non-Hermitian (NH) quasicrystals, describing systems with long-range order and with gain and loss or imaginary gauge fields, have attracted a considerable attention in recent research [3–26], particularly in the context of non-Hermitian topological physics and photonics [27, 28]. Non-Hermitian quasicrystals exhibit unique and exotic properties due to the combination of long-range order and non-Hermitian behavior. In particular, recent theoretical studies [3–7] have shown that certain NH variants of the Aubry-André model, a paradigmatic tight-binding model describing a one-dimensional quasicrystal, can feature a topological phase transition characterized by a spectral winding number. Remarkably, such a topological phase transition corresponds to a delocalization-localization transition and parity-time (PT) symmetry breaking phase transition as well [3]. Such as a coincidence of metal-insulator, PT symmetry-breaking and point-gap spectral topological phase transitions have been experimentally demonstrated in recent experiments based on quantum walks of photons in synthetic lattices [29, 30].

In non-relativistic wave equations, such as in the Schrödinger equation with continuous space and time, the physical phenomena are invariant under a Galilean transformation, which is reflected by the covariance of the Schrödinger equation for Galilean boosts [31]. This implies that any physical phenomenon, such as any phase transition, is not influenced by a relative motion of the underlying potential. However, on a lattice the discrete translational invariance of space, which results in a non-parabolic energy-momentum dispersion relation, breaks Galilean covariance [32–34]. This means that a relative motion between the underlying lattice and any superimposed potential can deeply affect the system behavior [32]. For example, it has been shown that the upper limit of velocity spreading in the lattice can make any potential scatteringless when drifting at a sufficiently fast speed [35, 36], and that Anderson localization can be washed out by a sufficiently fast sliding disorder [37]. An open question is whether topological phase transitions in NH quasicrystals can be observed when the incommensurate potential drifts on the lattice.

In this Letter we consider a NH quasicrystal, where the underlying NH incommensurate potential uniformly drifts at a speed v, and show that the topological phase transition is fully inhibited, even for arbitrarily small sliding velocities. Specifically, we show that the system is always in the topological trivial phase, corresponding to the delocalized phase and entirely real energy spectrum. Suppression of the topological phase transition in sliding NH quasicrystals can be explained by the inability of the drifting potential to dragg localized states. The results are illustrated by considering sliding photonic quasicrystals realized in fiber mesh lattices.

We consider wave dynamics on a lattice with a superimposed sliding incommensurate potential, uniformly drifting at a speed v, which is described by the discrete Schrödinger equation (see e.g. [32])

$$i\frac{\partial \psi}{\partial t} = -J[\psi(x+a,t) + \psi(x-a,t) - 2\psi(x,t)] + V(x-vt)\psi(x,t) \quad \textbf{(1)}$$

for the wave function $\psi = \psi(x,t)$, where a is the lattice period, J is the hopping amplitude and $V(x)$ is the incommensurate potential. Specifically, we will consider a NH incommensurate sinusoidal potential defined by [3]

$$V(x) = 2V_0 \cos(2\pi\alpha x/a + \theta + ih) \equiv 2V_0 \cos(2\pi\alpha x/a + \varphi) \quad \textbf{(2)}$$

where V_0 and $\varphi = \theta + ih$ are the amplitude and complex phase of the potential, respectively, and α is irrational Diophantine. As shown in Ref.[3], for the incommensurate potential at rest ($v = 0$) and for $J > V_0$ a topological phase transition, corresponding to a change of a spectral winding number w [38] and to the simultaneous delocalization-localization and PT symmetry breaking phase transitions, occurs as h is increased above the critical value

$$h_c = \ln\left(\frac{J}{V_0}\right). \tag{3}$$

Namely, for $h < h_c$ the energy spectrum is entirely real (unbroken PT phase) and all eigenstates are delocalized, corresponding to a trivial $w = 0$ spectral winding number, whereas for $h > h_c$ all eigenstates become exponentially localized and the energy spectrum becomes complex (broken PT phase), corresponding to a nontrivial winding number $w = \pm 1$ [3]. The non-vanishing winding number w in the broken PT phase is related to the formation of closed loops of the energy spectrum in complex plane; namely, w counts the number of times the complex spectral trajectory encircles any base point E_B, internal to any closed loop, when the real phase θ varies from zero to 2π (see Supplemental document for more technical details).
A main open and nontrivial question is whether such a phase transition persists for a sliding potential ($v \neq 0$). For a fast moving potential, we expect wave delocalization and thus suppression of the topological phase transition since the wave evolution on the lattice cannot follow the rapidly-oscillating incommensurate potential, which becomes scatteringless [35]. In fact, for $v \gg 2Ja/\alpha$ and taking into account that excitation on the lattice cannot spread at a speed faster than $\sim 2Ja$, at a given spatial coordinate x the potential $V(x,t)$ varies too fast in time to be followed by the wave on the lattice, so that on average it is washed out resulting in a potential-free lattice and delocalization: therefore, suppression of topological phase transition is expected for a fast sliding incommensurate potential. On the other hand, for a slowly-sliding potential one might expect that for $h > h_c$ the potential can adiabatically dragg all the exponentially-localized eigenstates of the system [37], in such a way that the topological phase transition is expected to be observable, may be at a shifted value of the critical parameter h_c. The main and rather unexpected result of this work is that the phase transition is fully suppressed even for an arbitrarily small sliding speed v, namely the system is always in the delocalized phase with an entirely real energy spectrum regardless of the value of the complex phase h. The main physical origin of phase transition suppression is ultimately rooted in the violation of Galilean invariance of the discrete Schrödinger equation (1) [32], i.e. the non-parabolic energy-momentum dispersion relation $E(p_x) = -2J[\cos(p_x a) - 1]$ in a lattice, and the inability of the moving incommensurate potential to dragg localized wave functions. In fact, if Eq.(1) were covariant for a Galilean boost, which occurs for a parabolic dispersion relation [32–34], the phase transition would be observable for an observer moving with the sliding incommensurate potential, since the localization features of any eigenfunction is not modified when changing the reference frame. The Galilean invariance in Eq.(1) is broken for any finite value of lattice period a, i.e. because of space discreteness. Only in the continuous-space approximation, defined by the double limit $a \to 0$ and $J \to \infty$ with $Ja^2 \equiv 1/(2m)$ finite (m is the effective mass in the parabolic approximation), the Galilean invariance is restored [32]; in this limiting case the energy-dispersion curve becomes parabolic, $E(p_x) \simeq Ja^2 p_x^2 = p_x^2/(2m)$, and clearly the topological phase transition is never reached since $J, h_c \to \infty$ and the system is always in the delocalized phase.
To prove that for a sliding incommensurate potential the system is always in the delocalized phase and the energy spectrum is entirely real, corresponding to a vanishing spectral winding number $w = 0$, let us rewrite Eq.(1) in the reference frame of the sliding potential. After letting $X = (x - vt)/a$, $T = t$ and $\Phi(X,T) = \psi(aX + vT, T)$ in Eq.(1), one obtains

$$i\frac{\partial \Phi}{\partial T} = \hat{K}\Phi(X,T) + V(aX)\Phi(X,T) \equiv \hat{H}\Phi(X,T) \tag{4}$$

where the kinetic energy operator $\hat{K}$ is given by $\hat{K} = -2J(\cos \hat{p}_X - 1) - (v/a)\hat{p}_X$ and where we have set $\hat{p}_X = -i\partial_X$. In the moving reference frame, the Hamiltonian $\hat{H} = \hat{K} + V(aX)$ is time independent, however unlike the continuous-space limit the additional term $(v/a)\hat{p}_X$ in the kinetic energy operator cannot be removed by any gauge transformation, indicating breakdown of the Galilean covariance of Eq.(1). The eigenfunctions $\phi(X)$ and corresponding energy spectrum E of $\hat{H}$, shifted by $2J$, are obtained from the spectral problem

$$E\phi(X) = -J[\phi(X+1) + \phi(X-1)] + i\frac{v}{a}\frac{d\phi}{dX} + V(aX)\phi(X) \tag{5}$$

with $V(aX) = 2V_0\cos(2\pi\alpha X + \theta + ih)$. As shown in the Supplemental document, for any $v \neq 0$ the eigenfunctions to Eq.(5) are extended waves and the energy spectrum entirely real independent of θ, regardless of the value of the complex phase h. This means that, even when h is much larger than h_c given by Eq.(3), the sliding incommensurate potential is not able to dragg the exponentially-localized eigenstates of the Hamiltonian at rest, even for extremely small drift velocities, resulting in the delocalization of the wave functions. Here we briefly outline the main steps of the proof, leaving the technical details to the Supplemental document. Owing to the periodicity of $V(aX)$ and since for $v \neq 0$ $\phi(X)$ should be a continuous differentiable function, we look for a solution to Eq.(5) of the Bloch form as a series expansion

$$\phi(X) = \sum_l \phi_l \exp(-i\mu X - i2\pi i\alpha l X), \tag{6}$$

where μ is an arbitrary parameter that varies in the range $(-\pi\alpha, \pi\alpha)$. This yields a set of difference equations for the spectral amplitudes ϕ_l. An extended state is found whenever $|\phi_l| \to 0$ fast enough as $l \to \pm\infty$, so that the series (6) is convergent. As shown in the Supplemental document, the spectral amplitudes ϕ_l display a Wannier-Stark localization, i.e. higher than any exponential, for $l \to \pm\infty$, regardless of the value of the complex phase h, and the energy spectrum is entirely real and independent of θ. This implies that the eigenfunctions are extended states and the winding number w trivially vanishes.

We checked the predictions of the theoretical analysis by direct numerical simulations of the discrete Schrödinger equation in the moving reference frame [Eq.(4)] using a standard pseudospectral split-step method. The solution to Eq.(4) for an infinitesimal propagation time step dT is written as $\Phi(X, T + dT) \simeq \exp(-idT\hat{K})\exp[-idTV(X)]\Phi(X,T)$; in the numerical simulations, the kinetic energy propagator term $\exp(-idT\hat{K})$ is computed in the Fourier (momentum) domain, while the potential term $\exp[-idTV(X)]$ is computed in physical space. Figures 1 and 2 show typical numerically-computed evolution of the wave function amplitude $|\Phi(X,T)|$, normalized at each time step to its norm, as obtained for a static (Fig.1) and slowly-drifting (Fig.2) potentials. The figures also depict the temporal

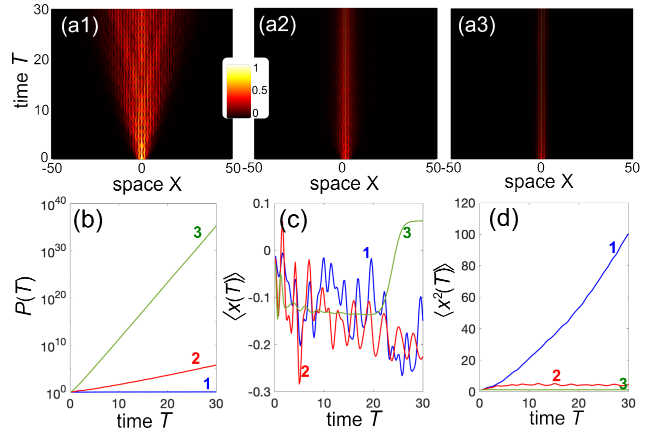

Fig. 1. Wave dynamics in the NH quasicrystal at rest. (a) Snapshots of wave evolution on a pseudocolor map (behavior of normalized wave amplitude $|\Phi(X,T)|$) for increasing values of the complex phase h: (a1) $h = 0.1$; (a2) $h = 0.5$; (a3) $h = 1$. Other parameter values are given in the text. The critical value h_c of the phase transition is $h_c = \ln(J/V_0) \simeq 0.223$. In (a1) the system is in the delocalized phase and the energy spectrum is real; in (a2) and (a3) the system is in the localized phase with complex energy spectrum. Panels (b), (c) and (d) show the temporal behavior of (a) the norm $P(T)$, (b) the wave packet center of mass $\langle X(T) \rangle$, and (d) the second moment $\langle X^2(T) \rangle$. Curves 1,2 and 3 refer to the three increasing values of h of panels (a).

behavior of the norm $P(T) = \int dX |\Phi(X,T)|^2$, wave packet center of mass $\langle X(T) \rangle = \int dX X |\Phi(X,T)|^2 / P(T)$ and second moment (variance) $\langle X^2(T) \rangle = \int dX (X - \langle X \rangle)^2 |\Phi(X,T)|^2 / P(T)$. Parameter values are $J = a = 1$, $\alpha = (\sqrt{5}-1)/2$, $\theta = 0$ and $V_0 = 0.8$, corresponding to a critical value $h_c = \ln(J/V_0) \simeq 0.223$ for the phase transition in the $v = 0$ case. As an initial condition, a narrow Gaussian wave function $\Phi(X,0) \propto \exp(-X^2/b^2)$ of size $b = 2$ has been assumed in the numerical simulations. For the static potential (Fig.1), a clear delocalization-localization phase transition is observed as h crosses the critical value h_c, with dynamical delocalization and a bounded norm for $h < h_c$, and dynamical localization with an unbounded norm for $h > h_c$, in agreement with previous studies [3]. For a sliding potential, even for a relatively small drift velocity ($v/a = 0.15$) no phase transitions are observed as h in increased far above h_c (Fig.2): wave delocalization is always observed with a norm which does not secularly grow. Figure 2(c) clearly indicates the inability of the sliding potential to dragg the wave function, since this would correspond to a locked (i.e. nearly time-independent) center of mass in the (X,T) reference frame.

Suppression of the topological phase transition in a sliding NH quasicrystal could be observed in different physical platforms of synthetic matter, such as ultracold atoms in quasi one-dimensional lattices and photonic quasicrystals. Here we consider photonic quantum walks [29, 30, 39, 40] in optical mesh lattices [40], which have been recently used for experimental demonstrations of topological phase transitions and mobility edges in NH quasicrystals [29, 30]. Unlike other kinds of synthetic matter, in such synthetic photonic lattices moving potentials can be readily implemented (see e.g. [41]). The system consists of two fiber loops of slightly different lengths that are connected by a fiber coupler with a coupling angle β. Phase

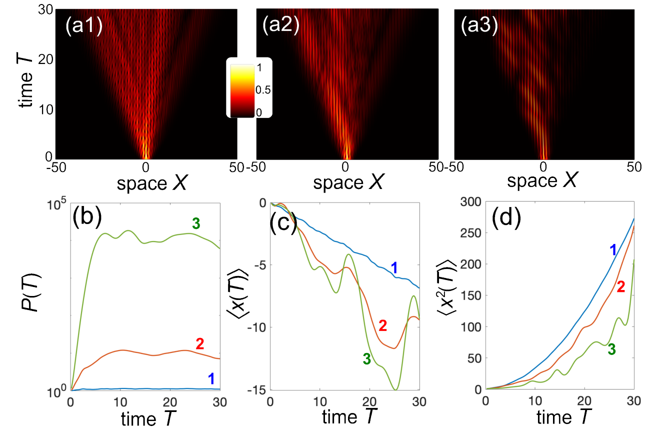

Fig. 2. Same as Fig.2, but for a slowly-drifting incommensurate potential at the speed $v/a = 0.15$.

and amplitude modulators are placed in one of the two loops, which provide a desired control of the phase and amplitude of the traveling pulses [40] that realize the sliding NH incommensurate potential. Light dynamics of optical pulses in the system is described by the set of discrete-time coupled-mode equations [29, 40–42]

$$u_n^{(m+1)} = \left(\cos\beta u_{n+1}^{(m)} + i \sin\beta v_{n+1}^{(m)} \right) \exp(-2i\phi_n^{(m)}) \quad (7)$$

$$v_n^{(m+1)} = \left(\cos\beta v_{n-1}^{(m)} + i \sin\beta u_{n-1}^{(m)} \right) \quad (8)$$

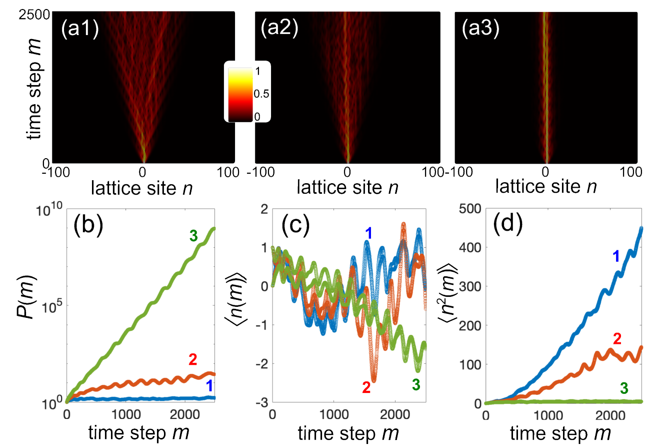

Fig. 3. (a) Light dynamics in a quasicrystal at rest realized in a synthetic mesh lattice for $\beta = 0.98 \times \pi/2$, $V_0 = 0.01$, $\theta = 0$, $\alpha = (\sqrt{5}-1)/2$ and for a few increasing values of the complex phase h: (a1) $h = 0.3$; (a2) $h = 0.5$, and (a3) $h = 0.7$. The critical value h_c of phase transition predicted in the continuous-time limit of the quantum walk is $h_c \simeq 0.4514$. Initial excitation of the lattice is $u_n^{(0)} = \delta_{n,0}$ and $v_n^{(0)} = 0$. In (a1) the system is in the delocalized phase with real energy spectrum, whereas in (a2) and (a3) the system is in the localized phase with complex energy spectrum. Panels (b), (c) and (d) show the temporal behavior of (b) the beam power $P(m)$, (c) the wave packet center of mass $\langle n(m) \rangle$, and (d) the second moment $\langle n^2(m) \rangle$. Curves 1,2 and 3 refer to the three increasing values of h.

where $u_n^{(m)}$ and $v_n^{(m)}$ are the pulse amplitudes at discrete time step m and lattice site n in the two fiber loops, and $2\phi_n^{(m)}$ com-

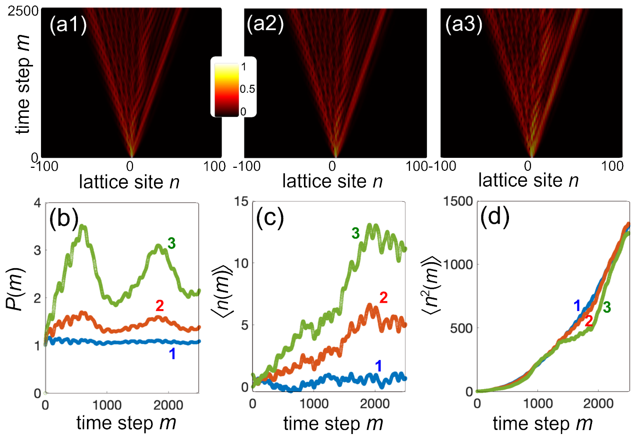

Fig. 4. Same as Fig.3, but for a sliding incommensurate potential with a drift velocity $v = 0.005$.

prises the phase and amplitude changes impressed by the modulators. A sliding NH incommensurate potential is realized by assuming $\phi_n^{(m)} = 2V_0 \cos(2\pi\alpha(n - mv) + ih)$ with $|v| \ll 1$. For a coupling angle β close to $\pi/2$ and for a weak modulation amplitude $V_0 \exp(h) \ll 1$, the light dynamics can be effectively described by the continuous-time model Eq.(1), with the discrete time m replaced by a continuous time variable $t = m$, $x = n$, $a = 1$ and with $J = \pm(1/2)\cos\beta$, $V(x,t) = \phi_n^{(m)}$ (for technical details see [42]). Wave spreading in the lattice is monitored by the time evolution of the second moment $\langle n^2(m)\rangle = \sum_n (n - \langle n(m)\rangle)^2 (|u_n^{(m)}|^2 + |v_n^{(m)}|^2)/P(m)$, where $P(m) = \sum_n (|u_n^{(m)}|^2 + |v_n^{(m)}|^2)$ is the beam power at time step m and $\langle n(m)\rangle = \sum_n n(|u_n^{(m)}|^2 + |v_n^{(m)}|^2)/P(m)$ is the beam center of mass. For the quasicrystal at rest ($v = 0$), the onset of the phase transition as h is increased above the critical value h_c can be experimentally observed by looking at the light dynamics for initial single-pulse excitation, $u_n^{(0)} = \delta_{n,0}$ and $v_n^{(0)} = 0$ [29]. An example of light dynamics for $v = 0$ is shown in Fig.3 for parameter values $\beta = 0.98 \times \pi/2$, $V_0 = 0.01$, $\alpha = (\sqrt{5} - 1)/2$ and $\theta = 0$. For such parameter values, the effective hopping rate J in the continuous-time limit is $J \simeq (1/2)\cos(\beta) \simeq 0.0157$, corresponding to a critical value $h_c = \ln(J/V_0) \simeq 0.4515$ for the phase transition. The figure clearly shows a phase transition, from a delocalized phase to a localized phase and with a corresponding qualitative different behavior of the beam power $P(m)$ related to the transition from an entirely real to a complex energy spectrum, as h is increased above the critical value h_c. For a sliding potential, the phase transition is suppressed and the system is always in the delocalized phase, as shown in Fig.4.

In conclusion, we predicted suppression of topological phase transitions in slowly-sliding NH quasicrystals, which is ultimately rooted in the violation of Galilean invariance of the discrete-space wave equation. Our results shed new physical insights onto the main role of Galilean invariance in the appearance of topological phase transitions in NH quasicrystals predicted and observe in recent works [29, 30], and indicate that light dynamics in synthetic mesh lattices could provide an experimentally accessible platform for the observation of phase transition suppression due to Galilean invariance violation.

Disclosures. The author declares no conflicts of interest.

Data availability. No data were generated or analyzed in the presented research.

Supplemental document. See Supplement 1 for supporting content.

REFERENCES

1. J. B. Suck, M. Schreiber, P. Häussler, Eds., *Quasicrystals: An Introduction to Structure, Physical Properties and Applications* (Springer, Berlin, 2002).
2. J. B. Sokoloff, Phys. Rep. **126**, 189 (1984).
3. 3. S. Longhi, Phys. Rev. Lett. **122**, 237601 (2019).
4. H. Jiang, L.-J. Lang, C. Yang, S.-L. Zhu, and S. Chen, Phys. Rev. B **100**, 054301 (2019).
5. Q.-B. Zeng and Y. Xu, Phys. Rev. Research **2**, 033052 (2020).
6. Q. Zeng, Y. Yang, and Y. Xu,Phys. Rev. B **101**, 020201(R) (2020).
7. S. Longhi, Phys. Rev. B **100**, 125157 (2019).
8. Y. Liu, X.-P. Jiang, J. Cao, and S. Chen, Phys. Rev. B **101**,174205 (2020).
9. T. Liu, H. Guo, Y. Pu, and S. Longhi, Phys. Rev. B **102**, 024205 (2020).
10. X. Cai, Phys. Rev. B **103**, 014201 (2021).
11. L. Tang, G. Zhang, L. Zhang, and D. Zhang, Phys. Rev. A **103**, 033325 (2021).
12. L. Zhai, G. Huang, and S. Yin, Phys. Rev. B **104**, 014202 (2021).
13. L. Zhou, Phys. Rev. Research **3**, 033184 (2021).
14. S. Longhi, Opt. Lett. **47**, 2951 (2022).
15. S. Longhi, Phys. Rev. B **103**, 054203 (2021).
16. Y. Liu, Q. Zhou, and S. Chen, Phys. Rev. B **104**, 024201 (2021).
17. X. Cai, Phys. Rev. B **103**, 214202 (2021).
18. S. Longhi, Phys. Rev. B **103**, 224206 (2021).
19. A. P. Acharya, A. Chakrabarty, and D. K. Sahu, Phys. Rev. B **105**, 014202 (2022).
20. L. Zhou and Y. Gu, J. Phys.: Condens. Matter **34**, 115402 (2022).
21. W. Han and L. Zhou, Phys. Rev. B **105**, 054204 (2022).
22. X. Cai, Phys. Rev. B **106**, 214207 (2022).
23. W. Chen, S. Cheng, J. Lin, R. Asgari, and X. Gao, Phys. Rev. B **106**, 144208 (2022).
24. L.-M. Chen, Y. Zhou, S. A. Chen, and P. Ye, Phys. Rev. B **105**, L121115 (2022).
25. S. Longhi, Phys. Rev. B **108**, 075121 (2023).
26. L. Zhou, Phys. Rev. B **108**, 014202 (2023).
27. A. Banerjee, R. Sarkar, S. Dey, and A. Narayan, J. Phys.: Cond. Matter **35**, 333001 (2023).
28. Q. Yan, B. Zhao, R. Zhou, R. Ma, Q. Lyu, S. Chu, X. Hu, and Q. Gong, Nanophoton. **12**, 2247 (2023).
29. S. Weidemann, M. Kremer, S. Longhi and A. Szameit, Nature **601**, 354 (2022).
30. Q. Lin, T. Li, L. Xiao, K. Wang, W. Yi, and P. Xue, Phys. Rev. Lett. **129**, 113601 (2022).
31. G. Rosen, Am. J. Phys. **40**, 683 (1972).
32. S. Longhi, EPL **120**, 20007 (2017).
33. K. A. Matveev and A. V. Andreev, Phys. Rev. B **100**, 035418 (2019).
34. P. Sharma, A. Principi, and D.L. Maslov, Phys. Rev. B **104**, 045142 (2021).
35. S. Longhi, Opt. Lett. **42**, 3229 (2017)
36. S. Longhi, Opt. Lett. **47**, 4091 (2022).
37. C. Guo, W. Cui, and Z. Cai, Phys. Rev. A **107**, 033330 (2023).
38. Z. Gong, Y. Ashida, K. Kawabata, K. Takasan, S. Higashikawa, and M. Ueda, Phys. Rev. X **8**, 031079 (2018).
39. A. Schreiber, K. N. Cassemiro, V. Potocek, A. Gabris, P. J. Mosley, E. Andersson, I. Jex, and C. Silberhorn, Phys. Rev. Lett. **104**, 050502 (2010).
40. A. Regensburger, C. Bersch, M. A. Miri, G. Onishchukov, D. Christodoulides, and U. Peschel, Nature **488**, 167 (2012).
41. H. Ye, C. Qin, S. Wang, L. Zhao, W. Liu, B. Wang, S. Longhi, and P. Lu, Proc. Nat. Acad. Sci. **120**, e2300860120 (2023).
42. S. Longhi, Opt. Lett. **48**, 5293 (2023).

References with full titles

1. J. B. Suck, M. Schreiber, P. Häussler, Eds., *Quasicrystals: An Introduction to Structure, Physical Properties and Applications* (Springer, Berlin, 2002).
2. J. B. Sokoloff, Unusual band structure, wave functions and electrical conductance in crystals with incommensurate periodic potentials, Phys. Rep. **126**, 189 (1984).
3. S. Longhi, Topological Phase Transition in non-Hermitian Quasicrystals, Phys. Rev. Lett. **122?**, 237601 (2019).
4. H. Jiang, L.-J. Lang, C. Yang, S.-L. Zhu, and S. Chen, Interplay of non-Hermitian skin effects and Anderson localization in nonreciprocal quasiperiodic lattices, Phys. Rev. B **100**, 054301 (2019).
5. Q.-B. Zeng and Y. Xu, Winding numbers and generalized mobility edges in non-Hermitian systems, Phys. Rev. Research **2**, 033052 (2020).
6. Q. Zeng, Y. Yang, and Y. Xu, Topological phases in non-Hermitian Aubry-André-Harper models, Phys. Rev. B **101**, 020201(R) (2020).
7. S. Longhi, Metal-insulator phase transition in a non-Hermitian Aubry-André-Harper model, Phys. Rev. B **100**, 125157 (2019).
8. Y. Liu, X.-P. Jiang, J. Cao, and S. Chen, Non-Hermitian mobility edges in one-dimensional quasicrystals with parity-time symmetry, Phys. Rev. B **101**,174205 (2020).
9. T. Liu, H. Guo, Y. Pu, and S. Longhi, Generalized Aubry-André self-duality and mobility edges in non-Hermitian quasiperiodic lattices, Phys. Rev. B **102**, 024205 (2020).
10. X. Cai, Boundary-dependent self-dualities, winding numbers, and asymmetrical localization in non-Hermitian aperiodic one-dimensional models, Phys. Rev. B **103**, 014201 (2021).
11. L. Tang, G. Zhang, L. Zhang, and D. Zhang, Localization and topological transitions in non-Hermitian quasiperiodic lattices, Phys. Rev. A **103**, 033325 (2021).
12. L. Zhai, G. Huang, and S. Yin, Cascade of the delocalization transition in a non-Hermitian interpolating Aubry-André-Fibonacci chain, Phys. Rev. B **104**, 014202 (2021).
13. L. Zhou, Floquet engineering of topological localization transitions and mobility edges in one-dimensional non-Hermitian quasicrystals, Phys. Rev. Research **3**, 033184 (2021).
14. S. Longhi, Non-Hermitian topological mobility edges and transport in photonic quantum walks, Opt. Lett. **47**, 2951 (2022).
15. S. Longhi, Phase transitions in a non-Hermitian Aubry-André-Harper model, Phys. Rev. B **103**, 054203 (2021).
16. Y. Liu, Q. Zhou, and S. Chen, Localization transition, spectrum structure, and winding numbers for one-dimensional non-Hermitian quasicrystals, Phys. Rev. B **104**, 024201 (2021).
17. X. Cai, Localization and topological phase transitions in non-Hermitian Aubry-Andrè-Harper models with p-wave pairing, Phys. Rev. B **103**, 214202 (2021).
18. S. Longhi, Non-Hermitian Maryland model, Phys. Rev. B **103**, 224206 (2021).
19. A. P. Acharya, A. Chakrabarty, and D. K. Sahu, Localization, PT-Symmetry Breaking and Topological Transitions in non-Hermitian Quasicrystals, Phys. Rev. B **105**, 014202 (2022).
20. L. Zhou and Y. Gu, Topological delocalization transitions and mobility edges in the nonreciprocal Maryland model, J. Phys.: Condens. Matter **34**, 115402 (2022).
21. W. Han and L. Zhou, Dimerization-induced mobility edges and multiple reentrant localization transitions in non-Hermitian quasicrystals, Phys. Rev. B **105**, 054204 (2022).
22. X. Cai, Localization transitions and winding numbers for non-Hermitian Aubry-André-Harper models with off-diagonal modulations, Phys. Rev. B **106**, 214207 (2022).
23. W. Chen, S. Cheng, J. Lin, R. Asgari, and X. Gao, Breakdown of the correspondence between the real-complex and delocalization-localization transitions in non-Hermitian quasicrystals, Phys. Rev. B **106**, 144208 (2022).
24. L.-M. Chen, Y. Zhou, S. A. Chen, and P. Ye, Quantum entanglement of non-Hermitian quasicrystals, Phys. Rev. B **105**, L121115 (2022).
25. S. Longhi, Phase transitions and bunching of correlated particles in a non-Hermitian quasicrystal, Phys. Rev. B **108**, 075121 (2023).
26. L. Zhou, Non-Abelian generalization of non-Hermitian quasicrystals: PT-symmetry breaking, localization, entanglement, and topological transitions, Phys. Rev. B **108**, 014202 (2023).
27. A. Banerjee, R. Sarkar, S. Dey, and A. Narayan, Non-Hermitian topological phases: principles and prospects, J. Phys.: Cond. Matter **35**, 333001 (2023).
28.Q. Yan, B. Zhao, R. Zhou, R. Ma, Q. Lyu, S. Chu, X. Hu, and Q. Gong, Advances and applications on non-Hermitian topological photonics, Nanophoton. **12**, 2247 (2023).
29. S. Weidemann, M. Kremer, S. Longhi and A. Szameit, Topological triple phase transition in non-Hermitian Floquet quasicrystals, Nature **601**, 354 (2022).
30. Q. Lin, T. Li, L. Xiao, K. Wang, W. Yi, and P. Xue, Topological Phase Transitions And Mobility Edges in Non-Hermitian Quasicrystals, Phys. Rev. Lett. **129**, 113601 (2022).
31. G. Rosen, Galilean Invariance and the General Covariance of Nonrelativistic Laws, Am. J. Phys. **40**, 683 (1972).
32. S. Longhi, Bound states of moving potential wells in discrete wave mechanics, EPL **120**, 20007 (2017).
33. K. A. Matveev and A. V. Andreev, Two-fluid dynamics of one-dimensional quantum liquids in the absence of Galilean invariance, Phys. Rev. B **100**, 035418 (2019).
34. P. Sharma, A. Principi, and D.L. Maslov, Optical conductivity of a Dirac-Fermi liquid, Phys. Rev. B **104**, 045142 (2021).
35. S. Longhi, Reflectionless and invisible potentials in photonic lattices, Opt. Lett. **42**, 3229 (2017).
36. S. Longhi, Invisible non-Hermitian potentials in discrete-time photonic quantum walks, Opt. Lett. **47**, 4091 (2022).
37. C. Guo, W. Cui, and Z. Cai, Localization of matter waves in lattice systems with moving disorder, Phys. Rev. A **107**, 033330 (2023).
38. Z. Gong, Y. Ashida, K. Kawabata, K. Takasan, S. Higashikawa, and M. Ueda, Topological Phases of Non-Hermitian Systems, Phys. Rev. X **8**, 031079 (2018).
39. A. Schreiber, K. N. Cassemiro, V. Potocek, A. Gabris, P. J. Mosley, E. Andersson, I. Jex, and C. Silberhorn, Photons Walking the Line: A Quantum Walk with Adjustable Coin Operations, Phys. Rev. Lett. **104**, 050502 (2010).
40. A. Regensburger, C. Bersch, M. A. Miri, G. Onishchukov, D. Christodoulides, and U. Peschel, Parity-time synthetic photonic lattices, Nature **488**, 167 (2012).
41. H. Ye, C. Qin, S. Wang, L. Zhao, W. Liu, B. Wang, S. Longhi, and P. Lu, Reconfigurable refraction manipulation at synthetic temporal interfaces with scalar and vector gauge potentials, Proc. Nat. Acad. Sci. **120**, e2300860120 (2023).
42. S. Longhi, Delocalization of light in photonic lattices with unbounded potentials, Opt. Lett. **48**, 5293 (2023).